The Drosophila ovarian terminal filament imports molecules needed to produce lipid droplets, the fusome, and functional germ cells

Bhawana Maurya and Allan C Spradling

[1]Howard Hughes Medical Institute Research Laboratory

Carnegie Institution for Science, Department of Biospherics

3420 San Martin Dr., Baltimore, MD 21212

ABSTRACT

Insect ovarioles typically begin with a protruding stack of flat cells known as the terminal filament (TF) located just upstream from germline stem cells (GSCs) in the germarium. However, terminal filament function has not been clearly established. We selectively knocked down genes only in TF cells using GAL4 driven by the TF-specific transcription factor *bric-a-brac 1 (bab1).* TF-specific loss of transporters or vesicle trafficking genes showed that terminal filament cells import molecules, transfer them through the cellular stack, and deposit near the GSC niche, a process required for ongoing oocyte production and to generate germ cell lipid droplets and fusomes. Loss of organic anion transporter Oatp30B in the TF blocked the development of GSC daughters (cystoblasts), implicating the TF in importing molecules needed for cyst and oocyte development, possibly including an endogenous ouabain. These experiments show the terminal filament imports lipids into the ovary, and is essential for germ cell development =[]]"""""and oocyte production.

INTRODUCTION

Ovaries in most insect species are divided into ovarioles containing germline cysts and ovarian follicles lined up in developmental order, like an assembly line (reviewed in Büning, 1994). Characteristically, each ovariole starts with a "terminal filament (TF)," described in the earliest study of an insect ovary by Malphigi in 1669 (see Gall, 1996) but whose functional significance has remained unclear (Figure 1A). TF cells are flattened like a stack of coins, but vary greatly in number between species (Sarikaya et al. 2011). They were commonly proposed to act as a "ligament" to mechanically anchor the ovary and its ovarioles to the abdominal wall. In *Campodea aquilonaris*, each TF starts at a cluster of fat body (Büning, 1994).

Currently, a role in germline stem cell (GSCs) niche development during the pupal stage represents the clearest TF function, while an unknown ongoing function in adulthood is only suspected. GSCs reside just below the TF in many species, and pupal TFs participate in niche establishment via Notch signaling that quantitatively influences cap cells development. 2-3 cap cells are required to hold and regulate each GSC the niche can support (Song et al. 2007). After the niche has formed, an ongoing role for the TF is less clear. Some insects that produce a very large number of offspring, like honeybee (*A. mellifera)* queens, contain TFs with 10 times more flat TF cells than are found in the Drosophila TF. Queens produce about twice as many eggs per ovariole per day over a lifespan that is 15-20 times longer than Drosophila females (Cullen et al 2024) suggesting greater ovariole activity or longevity might require a more robust TF. Honeybee terminal filaments preside over about 20 8-cell, fusome-containing germline cysts that function as GSCs. GSC-like cysts do not decline in number with age, but TF action seems to work at a distance because they only divide in the middle of the GSC region (Cullen et al 2024).

The well-studied Drosophila TF contains 8-9 flattened somatic cells that protrude from the end of each ovariole anteriorly, while the posterior ends contact the germline stem cell (GSC) niche (Figure 1A). With 5 or more cap cells (Figure 1A, yellow) and at least 4 special escort cells (Figure 1A, blue) these niches typically house and adhere strongly with two GSCs. Each GSC contain a large spherical spectrosome (Figure 1B-C), that located near the site of cap cells contact during most of the GSC cell cycle and upon division nucleates a fusome in daughter cystoblasts (deCuevas and Spradling, 1998). The niche constitutes a signaling hub that maintains GSC identity by secreting Bone Morphogenetic Protein (BMP) ligands including Decapentaplegic (Dpp) that inhibit GSC development. Daughter "cystoblasts" begin developing as they move away from the TF-cap cell region. The cystoblast starts 4 rounds of synchronous mitotic divisions and the resulting16-cell cysts enter meiosis and join a parade of sequentially older cysts. Cysts interact with additional stable squamous escort cells until about halfway through the germarium when they acquire epithelial stem cell (FSC)-derived follicle cells (Figure 1A, green) that grow to encase them in a monolayer shortly before they bud from the germarium as a new follicle (Hinnant et al. 2020).

Terminal filaments play additional roles in ovary differentiation in addition to constructing GSC niches. TFs represent the first evidence of ovariole formation in the third instar larval ovary, when TF cell precursors anterior to the germ cells migrate and intercalate in a spatially and temporally graded fashion along the medial-lateral axis to form 15-20 TF stacks (King et al. 1968; King, 1970; Godt and Laski, 1995; Sahut-Barnola et al. 1995). TF precursors begin to express two similar and essential BTB domain transcription factors *bric-a-brac 1* and *2 (bab1 and bab2)* prior to stack formation (Godt and Laski, 1995). L3 larval TF cells also express the signaling molecule *hedgehog (hh)* (Forbes et al. 1996). Drosophila terminal filament structure

changes during adulthood (Forbes et al. 1996). Over the first two weeks post eclosion, basal TF cells remain associated with the cap cells and maintain hh expression, but a gap sometimes forms between them and the more anterior cells that shut off hh.

We carried out genetic knockdown experiments (using bab1-GAL4) both throughout development and in adulthood (using also GAL80ts). This allowed us to show that terminal filaments serve continuously as a source of molecules, especially lipids, using precursors that are likely taken up from the hemolymph, including by the Oatp30B putative steroid receptor. When vesicle trafficking is selectively knocked down, transport that normally occurs through the TF stack is blocked leading to a build up of lipids in TF and cap cells. TF-dependent vesicle trafficking and transporter activity are essential for the normal production of germ cell lipid droplets, fusomes, cyst development, and directly or indirectly for GSC activity. The observed requirement for the Oatp30B transporter in TF cells for cystoblast development raises the question of whether endogenous ouabain, a novel steroid substrate, is imported by the TF and participates in ovariole regulation.

RESULTS

Lipid droplets and Hts-rich vesicles are found in terminal filaments

First, we looked for cellular components of germ cells in the vicinity of the TF that might be supported by its activities. We identified lipid droplets (LDs), including a few of substantial size, in each early germ cell by staining with BODIPY 493 or Nile red (Figure1B-E). They were also labeled with LipidTox, neutral lipid dyes that specifically mark lipids stored within LDs (Figure 1B-F). LDs were also consistently detected in TF cells from day 1 to day 8 post-eclosion (Figure 1B, C). TF LDs were relatively small, with diameters less than 0.3 µm and were easily overlooked, whereas substantially larger LDs were found in germ cells (Figure 1D, E). It was

not clear whether TF cells synthesized or acquired these lipid components or whether they transport them to other cells.

We also detected structures enriched in protein isoforms produced by the *hu-li tai shao (hts)* gene specifically within TF cells of newly eclosed flies (day 0–1). Hts-staining is normally observed in germ cell fusomes, and due to a different, adducin-like Hts isoform, also underneath plasma membranes (Petrella et al, 2007). GSCs and forming cysts greatly expand the amount of fusome they contain during their residence in the germarium but sources of fusome materials other than internal biosynthesis have not been identified. TF-resident Hts-positive structures (Figure 1B, triangle) were small, from 0.2 to 1.2 µm in size, much smaller than spectrosomes and fusomes in GSCs and downstream germ cells. Fusomes are produced continuously while cysts are growing in the germarium. In sharp contrast, small Hts-positive vesicles in TF cells were only found during day 1-2. This restricted time frame suggested that they are related to the earliest "wave" of follicles termed "wave 1." These follicles arise during pupal development directly from PGCs rather than GSCs (Zhu and Xie, 2003; Asaoka and Lin, 2004) and are laid as eggs during the first few days under laboratory conditions.

Terminal filament cells transport lipids to germ cells via exocyst-dependent vesicle trafficking

The exocyst complex represents a key regulator of polarized exocytosis, and is responsible for tethering secretory vesicles to specific plasma membrane domains prior to fusion. If TF cells exchange lipids with cap cells that ultimately appear in germ cells, the exocyst would almost certainly be required (review: Meek et al. 2024). Although the exocyst is used by most or all cells, and is critical for cytokinesis in mitotically cycling cells, adult TF cells do not cycle or divide and appear fully differentiated. Sec6 is a key exocyst component due to its binding to Rab9 at the plasma membrane and to Rtn1 in the ER (Morgera et al. 2012). Consequently, we

used the TF-specific driver *bab1-GAL4*, the GAL80ts GAL4 repressor, and a UAS- Sec6 RNAi construct to knockdown expression of Sec6 with temporal and cell type-specific control. To validate the experimental approach we showed that in the absence of RNAi there was no effect on ovary morphology Figure 2A or lipid droplets (Figure 2D). In the presence of UAS-sec6 RNAi egg laying was strongly reduced (Figure 2B,C), and lipid droplets were nearly absent from the anterior germarium (Figure 2E, F).

To provide insight into the timing of , we limited the knockdown not only to terminal filament cells, but also to a specific interval of adulthood using *bab1-GAL4, tub-Gal80^{ts}*. Females were initially maintained at 18 °C to allow Gal80^{ts} mediated repression of Gal4 activity, then shifted to 29 °C to inactivate Gal80^{ts} and induce RNAi knockdown after TF morphogenesis was complete. Under these conditions, *Sec6* knockdown in TFs led to a marked reduction in LD levels throughout the germarium, as revealed by BODIPY 493/503 staining (Figure 2D–E). Quantification showed a significant decrease in LD number compared to controls (Figure 2F).

Interestingly, while LDs were depleted from germ cells, we observed an accumulation of large LDs specifically within the TF and cap cells in *sec6* knockdown compared to control (Figure 2 G-H). Quantitative analysis confirmed a significant increase in LD size and number in the TF region (Fig2 I). This phenotype suggests that under normal conditions, the TF acts as a source of lipid delivery to germ cells. When exocytosis is disrupted, lipids may accumulate in the TF due to impaired vesicular trafficking and secretion, leading to a lipid backup within the niche cells. These findings highlight a previously unrecognized function of the TF as a lipid transport hub that supports germline development.

<u>Knockdown of other exocyst components also affect lipid vesicle trafficking:</u>

Similarly, knockdown of other exocyst components (*Sec5*, *Sec15*, *Sec10*, *Exo70*, *Exo84*) also resulted in LD depletion in the germarium (Fig 2J-O, P), though the *Sec6* knockdown produced the most severe phenotype, with near-complete LD loss. It was surprising that these knockdowns showed much less backup of LDs in the TF, yet they still fully impaired the accumulation of LDs throughout the germarium after several days. This suggested that germ cells display a high ongoing requirement for lipids, and that lipid mobility within the germarium may be much more rapid than the relatively slow movement of germ cells themselves. Lipids are not simply loading into the germ cells located adjacent to the TF and cap cells, and then moving along with cells to the posterior. Lipids seem able to move into and out of germ cells with much more rapid kinetics throughout the anterior germarium.

Lipid and cytoskeletal protein transport from terminal filament support germ cell and cyst development:

To examine how disrupted trafficking from the terminal filament affects germ cell development, we again performed *Sec6* knockdown in TF cells using *bab1-GAL4, tub-GAL80^{ts}* flies. Flies were shifted to 29 °C at the late pupal stage, long after TF morphogenesis is complete and dissected at various time points post-eclosion (days 2, 4, 6, and 8). In these conditions, lipid droplets (LDs) consistently accumulated in the TF, while LD levels in the germarium were significantly reduced throughout all observed time points (Figure 3A–G). Quantitative analysis confirmed that lipid accumulation in the TF persisted across all days assessed, indicating a stable transport defect. Since under our conditions, the age dependent changes in the TF were detected by day 8 post-eclosion, (Figure 1B,C), we further assessed the persistence of the LD depletion phenotype during TF aging. Analysis of *Sec6* knockdown flies from day 1 to day 30 revealed

that LD accumulation in the TF remained consistent, suggesting that the lipid transport capacity of TF is not altered by age (Figure S1).

In addition to lipid accumulation, *Sec6* knockdown in TFs led to the formation of Hts-positive aggregates, which were not observed in controls and remained detectable throughout days 2 to 8 post-eclosion (Figure 3A'-E'). Quantification showed a progressive increase in both the number and size of Hts aggregates in TFs (Fig3 J,K). The accumulation of Hts aggregates within TFs suggests that TF cells contribute a substantial volume of Hts-containing precursors to germ cells under normal conditions. However, the backup and altered accumulation of these fusome materials led to defects in GSC spectrosome morphology and in fusome organization within cysts (Fig3, A-E, A'-E'). Similarly downregulating other exocyst components, including *Exo84, Exo70*, *Sec10*, *Sec15*, and *Sec5* resulted in Hts aggregate formation in TF along with small spectrosome formation (Fig S2). From day 4 onward, these morphological defects were accompanied by disrupted follicle formation, indicating that defective fusome formation strongly impairs downstream cyst and follicle development (Figure 3A–E).

To investigate whether escort cells also participate in lipid delivery, we knocked down *Sec6* using the escort cell-specific driver *c587-GAL4*. [Note: c587 also drives expression in FSCs and early follicle cells; so c587-driven sec6 depletion is expected to also impact follicle cells]. The experiment also altered cyst development and impaired follicle formation (Figure 3 O,P). However, these effects were much milder that the effects of bab1-driven knockdown, and consisted of a backup of region 2a follicles, followed by highly abnormal region 2b follicles, which is the expected result of disrupting follicle cell proliferation by the loss of exocyst activity in their mitotic cycles. Unlike after TF knockdown of sec6, LD levels in germ cells following c587-driven KD were not significantly reduced (Figure 3Q). We conclude that escort cells do

not make a substantial contribution to the supply of germ cell lipids and fusome materials. Rather, the TF and cap cells appear to be the main lipid-donating somatic cells in the anterior germarium.

To confirm active exocytosis in TF and cap cells, we used FM1-43 dye, which labels vesicles undergoing membrane recycling and regulated exocytosis. FM1-43 is widely used in studies of synaptic activity and neurogenesis, where it marks vesicle turnover during neurotransmitter release. In control ovarioles, FM1-43 strongly labeled vesicles in TF and cap cells, indicating robust exocytic activity (Figure 3L). In contrast, *Sec6* knockdown significantly reduced FM1-43 signal in these regions, consistent with impaired vesicle recycling and secretion (Figure 3M). These observations reinforce the functional requirement of the exocyst complex for lipid vesicle trafficking in TF cells.

Terminal filament express transporters that influence germ cell development

We looked for genes expressed in terminal filament (TF) in scRNAseq libraries that might support the functions identified here in lipid and fusome production (Slaidina et al. 2020; Sladina et al. 2021). Since acquisition of lipids to transport from hemolymph seems likely to be essential, we identified multiple transporters and channels that are expressed by TF cells (Table 1) suggesting these cells may take up and transport organic solutes, lipids, ions, and small molecules.

We focused initially on the organic anion transporting polypeptide 30B (Oatp30B)**,** a member of the Oatp30B which is strongly and specifically expressed in the terminal filament in adult Drosophila as shown by the enhancer trap line (PZ00078; Figure 4A).

To see if Oatp30B had a function in this system, we specifically knocked down Oatp30B in TF cells using bab1-GAL4. Disruption of Oatp30B function in TF cells caused a marked

reduction in lipid droplet levels within the germarium (Figure 4B–E), indicating that *Oatp30B* contributes to lipid delivery or uptake in developing germ cells. In addition to lipid reduction, Oatp30B knockdown also resulted in differentiation defects in the germline. Normally, spectrosomes are restricted to germline stem cells, and serve as a marker for GSCs and their daughter cystoblasts (CBs). Normally, the anterior germarium contains about 3 spectrosome-containing cells (Figure 4B), however, after shifting bab11GAL4. GAL80ts ; UAS-Oatp30B_RNAi flies to the restrictive temperature for 3 days caused an accumulation of 7-8 cells containing spectrosomes per germarium, largely filling the space up to region 2A (Figure 4C, E). This shows that GSC activity continued but germ cell development beyond the GSC was arrested

Oatp30B is a candidate transporter for the cardiac glycoside ouabain, which acts by inhibiting the Na^+/K^+-ATPase and locking it in a non-functional conformation. Evidence for production of an endogenous source of a ouabain-like molecule has been obtained in both mammals (Laredo et al. 1995; El-Masri et al. 2002) and insects (Torrie et al. 2004) but a biosynthetic pathway has remained unclear. The Drosophila Na/K-ATPase alpha subunit contains a highly conserved ouabain binding site (Dostanic-Larson et al. 2005). Furthermore, immunostaining revealed that its target, Na^+/K^+-ATPase, is highly enriched in TF cells (Figure 4F, G). Strikingly, TF-specific knockdown of *Oatp30B* significantly reduced Na^+/K^+-ATPase expression (Figure 4H, I) suggesting that the uptake of small organic molecules via Oatp30B may regulate ion pump expression or stability in niche cells.

To investigate the downstream consequences of ion imbalance, we examined the status of Hedgehog (Hh) signaling, which is known to be regulated by membrane potential and ion flux in other tissues such as the wing disc (Liu et al., 2018). Hh signaling plays a critical role in TF

organization and stem cell niche maintenance. In controls, Hh expression was detected in TFs; however, in Oatp30B knockdown ovaries, Hh expression was markedly reduced (Figure 4J–L), indicating that disruption of Oatp30B and its downstream ionic balance may impair Hh-mediated niche signaling.

Lipid droplets in the germarium protect against mitochondrial ROS accumulation:

Why does the germarium require a continuous supply of lipids, and do LDs serve functions beyond energy storage? We have observed that LDs in early germ cells are frequently in close proximity to mitochondria in the germarium (Figure 5A). This spatial association is consistent with earlier reports suggesting that LD–mitochondria contacts facilitate fatty acid transfer**,** enabling mitochondrial respiration and regulating oxidative homeostasis (Nguyen et al., 2017; Rambold et al., 2015). Disruption of these contacts or LD content has been linked to elevated mitochondrial reactive oxygen species (ROS) and organelle dysfunction.

To directly test whether **l**oss of lipid droplets leads to ROS accumulation**,** we knocked down the lipogenic gene Acetyl-CoA Carboxylase (ACC) in germ cells using *nanos-GAL4*. ACC is a key enzyme in de novo fatty acid synthesis and is essential for neutral lipid production. ACC knockdown resulted in a dramatic reduction or complete loss of LDs throughout the germarium (Figure 5B–D). We next assessed mitochondrial ROS using MitoSOX and DHE staining. Both assays showed significantly elevated ROS levels in ACC-depleted germarium compared to controls (Figure 5E–F, H; I–J, L), indicating oxidative stress resulting from lipid depletion.

To determine whether this ROS phenotype also arises when LD transport from the TF is impaired, we examined TF-specific knockdown of *Sec6*. As previously shown, *Sec6* knockdown blocks vesicular transport of lipids to the germarium. Consistent with our hypothesis, *Sec6*-RNAi

in TFs also led to elevated mitochondrial ROS in germ cells, as measured by both MitoSOX and DHE (Figure 5E–G, H; I–K, L).

DISCUSSION

The terminal filament imports molecules from the hemolymph and transfers them into the ovariole to support GSCs and oocyte production

Our experiments demonstrate that a major function of the Drosophila terminal filament is to important lipids and other molecules into the GSC region where they can be deployed to support germ cell cyst and follicle development. The effects of losing genes related to TF import extended well beyond the immediate vicinity of its connection to the anterior germarium, however. Thus, TF import is coupled with a system for distributing lipids and other products it delivers. Large lipid droplets within germ cells were the most visible structures dependent on TF import. These molecules disappeared from the anterior germarium within a day of TF inhibition. The strong developmental conservation and unusual nature of this system compared to nutrient uptake in other insect tissues suggests is serves a special role in oocyte production.

Our experiments argued that lipids move much faster than the posterior movement of cells resulting from GSC-driven proliferation. When we blocked lipid transport within the TF and into the niche region by raising the temperature to inactivate GAL80, there was a rapid decrease in LDs within germ cells in throughout the anterior germarium without a clear gradient as expected if lipids loaded into germ cells near the TF while germ cells already containing LDs remained unaffected. Rather depletion developed rapidly, indicating that lipid continues to be transferred from cell to cell even after leaving the TF. The speed and efficiency of this process

probably explains why vesicles in transit in the terminal filament remain sparse under normal conditions Only when the strongest exocyst mutation was studied, sec6, did the population of lipid droplets in the TF start to build up substantially.

Import via the terminal filament may select for quality components

The strong dependence of ovarian lipid droplets in the early ovary on particular source may arise simply because there are few alternatives to the terminal filament for lipid acquisition in the ovariole anterior. However, there is a high flux of precursor molecules overall from the gut to the ovary under favorable environmental conditions. Drosophila females are able to lay a substantial fraction of their weight in eggs each day, a prodigious feat suggesting that internal ovarian transport is not likely to be rate limiting. More likely to be challenging than simple transport in producing gametes is the need for lipid quality imposed by germ cell rejuvenation, the elimination of modified lipids that catalyze errors that might begin to increase in subsequent generations. TF-derived lipids may be relied upon for example, because movement through the TF may involve a process of quality selection.

Lipids absorbed in the diet are typically distributed through the hemolymph as lipoprotein particles for uptake by cells for their use. Our findings suggest that early germ cells, which do not have direct access to the hemolymph but have a strong need for lipids for growth, do not simply take up lipids from the hemolymph on a cell autonomous basis like in many somatic tissues. The terminal filament appears to take up dietary lipids directly from hemolymph, and transfer them to germ cap cells and then to germ cells and possibly to niche cells somatic cells. When we strongly disrupted sec6 in the TF, a significant buildup of lipids occurred in multiple TF cells. This shows that multiple cells take up LDL particles and transport them from cell to

cell by endocytic trafficking, exocytosis, within multiple TF cells and then cap cells. At this point, transported products contact and may enter nto a GSC, cap cell, or into an escort cell, that contracts cap cells.

There are thousands of lipid species and many ways that they can become modified with innumerable possible adducts. To generate fresh membranes without a history of past modifications, germ cells may strive to resynthesize as many molecules as possible over in germ cells. This could lead them to use the TF to take up precursors and purify away all lipid contaminants as they move along the TF stack. Thus, the TF may function like a lipid column, purifying the incoming fatty acids, TGs etc. with the end result of supplying the GSC niche with the best possible materials for generating new plasma and organelle membranes.

TF-like interfollicular "stalk" cells may provide a similar function to follicles

Our findings also suggest a reason that follicles in ovarioles are connected by interfollicular stalks. Some of the most critical oocyte components such as organelles may be rebuilt in the germarium during the meiotic stages associated with rejuvenation in lower eukaryotes. Although the very best membranes might already have been used to reconstitute the organelles of the Balbiani body, additional organelles and membrane lipids are still needed in cytoplasm that will be used in somatic cells. The great majority of growth based on volume increase takes place after the first follicle has formed. Consequently, several additional ncell types with terminal filament,-like architecture, namely interfollicular stalk cells, may serve a related function as a source of input and quality control for the uptake of hemolymph lipoproteins. These smaller "filters" may still provide value in removing the alterations that are likely to be found in dietary lipids taken up directly from the gut or fat body. Finally, the

terminal web of the pupal ovary has one the longest sequence of TF-like cells, and it may provide nutrients at a critical time as the first follicles to derive from stem cells begin to appear.

The terminal filaments may regulate the metabolism and activity levels ovariole by ovariole

There is a large variation in the number of TF cells across diverse Drosophila species and among other insects (Sarikaya et al. 2011). However, there has been little progress in understanding how these difference arise and their biological significance due to the near absence of insight in to TF physiology. Our results suggest that the terminal filament plays a central role in controlling the overall rate of function of the ovary via its control of import of lipid precursors for membrane production, secretion and hormone import and storage. Positioned at the head of the ovary, in some ways like the location of the thyroid and pituitary glands near the origin of the gut, the TF is well located for ovary regulation. Major effectors of this control are likely steroid hormones (Morris and Spradling, 2011). The follicle cells produce and secrete ecdysone locally in follicles to coordinate cellular behavior that allows stage-specific development. Some estrogen likely is secreted into the hemolymph as the circulating level of estrogen is substantially higher in females than in males. This secretion is thought depend on insulin gut enteroendocrine peptides to ensure that the level of overall egg production matches the available resources. The terminal filament likely responds to these signals due to its proximity to the GSC niches, and ensures that GSC division and follicle production is maintained in all ovarioles..

Relatively little is known about how follicle development is coordinated to keep the same number and approximate stage distribution matched across 32 ovarioles spread across two ovaries. The terminal filament assisted by stalk cells and calyx cells at the base of the ovary, may help support and coordinate these processes. All the stem cells and downstream cells are used at

similar levels initially, but if one suffers delays or becomes stalled the activity of the others adjusts to maintain the output of the organ as a whole. This regulation continues up to ovulation, where there is efficient, equal usage of individual ovarioles using regulatory paradigms that have been conserved to mammals (Knapp and Sun, 2017; review; Berg et al. 2024).

Ovariole regulation by TFs may utilize a novel steroid regulator sensed by Oatp30B- endogenous oubain

The terminal filament may act by controlling the importation of regulatory steroid hormones. During pupal development, the TF highly expresses a different Oatp gene, Oatp74D, which has been shown to be capable of transporting ecdysone (Scanlan et al. 2023). In adults the TF highly expresses Oatp30B, which is closely related to the human importer SLC05A (Roshandel et al. 2023). We showed here that Oatp30B is required for normal female germ cell development downstream from the GSC. We did not see as strong an effect on GSC differentiation in exocyst disruptions in the TF, suggesting that movement of the Oatp30B substrate may not follow the same pathway in TF cells as LD precursors. In humans, SLC05A1 is thought to transport estrogen derivatives. Its prognostic value for better ovarian cancer outcomes may result from a role supporting continuing estrogen dependence of these tumors (Svoboda et al. 2018). A genetically tractable model of Oatp30B function in the ovary would be valuable for a better understanding of endogenous ouabain function in the mammalian and insect ovaries.

LDs may not serve merely as lipid storage depots but may function to maintain redox balance in early germ cells. LDs may buffer excess free fatty acids, distribute lipids to mitochondria in a regulated manner, and prevent lipotoxic stress. In the absence of LDs, free fatty acids can undergo peroxidation, triggering a cascade of oxidative damage (Listenberger et

al., 2003; Bailey et al., 2015). LDs are also important in the nervous system to protect against the deleterious effects of lipid peroxidation by transporting them to glial cells for removal (Moulton et al. 2021). Maintenance of this capacity could also contribute to cancer resistance.

METHODS

Fly Genetics

All *Drosophila melanogaster* stocks were maintained on standard cornmeal agar media at room temperature unless otherwise specified. The Oregon R strain was used as the wild-type control throughout the study. The GAL4 driver lines *bab1-GAL4*, *c587-GAL4*, and *nanos-GAL4* were obtained from the Bloomington Drosophila Stock Center (BDSC). UAS-RNAi lines were obtained from the Vienna Drosophila Resource Center (VDRC), including *Sec6-RNAi* (VDRC #22077), *Sec15-RNAi* (VDRC #35161), *Sec10-RNAi* (VDRC #318483), *Sec5-RNAi* (VDRC #28873), *Exo70-RNAi* (VDRC #103717), *Exo84-RNAi* (VDRC #108650), *Oatp30B-RNAi* (VDRC #110237), and *ACC-RNAi* (VDRC #8105). All genetic crosses were performed at 25 °C unless otherwise noted. For temporally controlled gene knockdown, the temperature-sensitive Gal80 system (*tub-GAL80^{ts}*) was used in combination with *bab1-GAL4*. Crosses were maintained at 18 °C to allow GAL80^{ts} mediated repression of GAL4 activity during development. Adult progeny was then shifted to 29 °C to inactivate GAL80^{ts} and permit GAL4 driven RNAi expression at desired developmental stages.

Egg Laying Assay

Newly eclosed (0–1 day old) flies were maintained in plastic bottles containing molasses plates overlaid with a layer of wet yeast, replaced daily. For egg laying measurements, five pairs of flies were kept per bottle, and the number of eggs laid was counted every 24 hours, in triplicate.

Immunostaining:

Immunostaining was performed on ovaries dissected from adult *Drosophila melanogaster* females. Dissections were carried out in Grace's insect medium, followed by fixation in 4% paraformaldehyde (PFA) with 0.01% PBST (PBS with 0.01% Triton X-100) for 30 minutes at

room temperature. Fixed ovaries were then blocked in 5% Normal Goat Serum (NGS) for 1 hour and incubated overnight at 4°C with primary antibodies diluted in blocking solution. After extensive washing with PBST, samples were incubated with secondary antibodies (1:200 dilution) for 2 hours at room temperature. DNA was counterstained with DAPI (0.5 µg/mL), and samples were mounted in Vectashield mounting medium. Confocal images were acquired using a Leica STELLARIS 8 DIVE microscope. Intensity profile graphs were generated using Image J (NIH) and GraphPad Prism software.

The following primary antibodies were used: mouse anti-Hts (1:100; DSHB), chicken anti-α5 (1:200; DSHB), mouse anti-LaminC (1:50; DSHB), rabbit anti-Cytochrome C (1:50; Cell Signaling Technology), and rabbit anti-Hedgehog (1:500; kindly provided by Dr. Tom Kornberg).

Nile Red, BODIPY 493/503 and LipidTOX™ Deep Red Staining

To visualize neutral lipids, tissues were dissected in 1× PBS and fixed in 4% paraformaldehyde for 20 minutes at room temperature. Samples were washed three times with 1× PBS and incubated in Nile Red solution (1 µg/mL in PBS), LipidTOX™ Deep Red (1:500), BODIPY 493/503 (1 µg/mL in PBS) for 30 to 45 minutes in the dark. After staining, tissues were washed briefly with PBS, counterstained with DAPI (0.5 µg/mL), and mounted in Vectashield for imaging. Images were acquired using a confocal microscope.

FM1-43 staining

Ovaries were dissected in ice-cold 1× PBS and incubated in FM1-43FX dye (5 µg/mL in PBS; Thermo Fisher) for 15–20 minutes at room temperature in the dark. After staining, tissues were washed briefly with PBS and fixed in 4% paraformaldehyde for 20 minutes. Following fixation, samples were washed three times with PBS and mounted in Vectashield for imaging.

DHE and MitoSox Staining

To assess reactive oxygen species (ROS) levels, freshly dissected ovaries were incubated in Schneider's Drosophila medium containing either dihydroethidium (DHE; 5µM, Invitrogen) or MitoSOX™ Red (5 µM, Invitrogen) for 10–15 minutes at room temperature in the dark. After staining, tissues were washed twice with 1× PBS and fixed in 4% paraformaldehyde for 20 minutes. Samples were then rinsed, mounted in Vectashield with DAPI, and imaged using a confocal microscope.

Statistical Analysis:

All experiments were performed in triplicate. Data were analyzed using GraphPad Prism version 10 and are presented as mean ± standard deviation (SD). Statistical significance was assessed using one-way ANOVA, with $p < 0.05$ considered significant.

ACKNOWLEDGEMENTS

We thank Mahmud Siddiqi for assistance with microscopy and Dianne Williams for help with Drosophila stock management. We are grateful to Madulika Pathak, Ashish Tiwari, Yunpeng Fu, Andy Mao and other members of the Spradling laboratory for discussions. Allan Spradling is an Investigator of the Howard Hughes Medical Institute who provided generous funding for this work. The Carnegie Institution for Science has generously supported the Spradling lab in Baltimore for many years, for which we remain grateful.

REFERENCES

Asaoka M, Lin H. (20040. Germline stem cells in the Drosophila ovary descend from pole cells in the anterior region of the embryonic gonad. Development 131, 5079-89. doi: 10.1242/dev.01391.

Bailey, A. P., et al. (2015). Antioxidant role for lipid droplets in a stem cell niche of *Drosophila*. *Cell*, **163**(2), 340–353.

Berg C, Sieber M, Sun J.(2024). Finishing the egg. Genetics. 226: iyad183. doi: 10.1093/genetics/iyad183.

Büning J. (1994). The Insect Ovary: Ultrastructure, Previtellogenic Growth and Evolution. Chapman and Hall. DOI:https://doi.org/10.1007/978-94-011-0741-9.

Cullen G, Delargy E, Dearden PK. (2024). Development of germline progenitors in larval queen honeybee ovaries. Biol Open. 13, bio060511. doi: 10.1242/bio.060511.

de Cuevas M, Spradling AC (1998) Morphogenesis of the Drosophila fusome and its implications for oocyte specification. Development 125:2781–2789. https://doi.org/10.1242/dev.125.15.2781

Dostanic-Larson I, Van Huysse JW, Lorenz JN, Lingrel JB. (2005). The highly conserved cardiac glycoside binding site of Na,K-ATPase plays a role in blood pressure regulation. Proc Natl Acad Sci U S A. 2005 Nov 1;102(44):15845-50. doi: 10.1073/pnas.0507358102. .

El-Masri MA et al. (2002). "The circulating ouabain-like factor is ouabain." *J Biol Chem* 277(6):388–395. DOI: 10.1074/jbc.M105980200

Forbes, Z., Lin, H., Ingham, P. and Spradling, A.C. (1996). *hedgehog* is required for the proliferation and specification of somatic cells prior to egg chamber formation in Drosophila. Development 122: 1125-1135.

Gall JG. (1996). Views of the the Cell: a pictorial history. American Society for Cell Biology Press.

Godt D, Laski FA. (1995). Mechanisms of cell rearrangement and cell recruitment in Drosophila ovary morphogenesis and the requirement of bric à brac. Development. 121, 73-87. doi: 10.1242/dev.121.1.173.

Hinnant, T. D., Merkle, J. A., & Ables, E. T. (2020). Coordinating Proliferation, Polarity, and Cell Fate in the Drosophila Female Germline. Frontiers in Cell and Developmental Biology 8, 19. https://doi.org/10.3389/FCELL.2020.00019.

King RC. (1970). Ovarian development in Drosophila melanogaster. Academic Press.

Knapp E, Sun J. (2017). Steroid signaling in mature follicles is important for Drosophila ovulation. Proc. Natl. Acad. Sci. U.S A., 114, 699-704, 10.1073/pnas.1614383114.

Laredo J et al. (1995). "Ouabain is secreted by bovine adrenocortical cells." *Endocrinology* 136(10):4873–4881

Liu, Y., et al. (2018). Ion channel modulation of Hedgehog signaling: a new mechanism for regulating morphogenesis and tissue patterning. *Developmental Cell*, **47**(3), 307–321. https://doi.org/10.1016/j.devcel.2018.10.004

Listenberger, L. L., et al. (2003). Triglyceride accumulation protects against fatty acid-induced lipotoxicity. *Proceedings of the National Academy of Sciences*, **100**(6), 3077–3082.

Meek S, Hernandez AC, Oliva B, Gallego O. (2024). The exocyst in context. Biohemical Society Transactions 52, 2113-22.

Morgera F, Sallah MR, Dubuke ML, Gandhi P, Brewer DN, Carr CM, Munson M. (2012). Regulation of exocytosis by the exocyst subunit Sec6 and the SM protein Sec1. Mol Biol Cell. 23, 337-46. doi: 10.1091/mbc.E11-08-0670.

Moulton MJ, Barish S, Ralhan I, Chang J, Goodman LD, Harland JG, Marcogliese PC, Johansson JO, Ioannou MS, Bellen HJ. (2021). Neuronal ROS-induced glial lipid droplet formation is altered by loss of Alzheimer's disease-associated genes. Proc Natl Acad Sci U S A. 118, e2112095118. doi: 10.1073/pnas.2112095118.

Morris, L., and Spradling, A.C. (2011). Long-term live imaging provides new insight into stem cell regulation and germline-soma coordination in the Drosophila ovary. Development 138, 2207-2215. doi: 10.1242/dev.065508

Nguyen, T. B., et al. (2017). DGAT1-Dependent Lipid Droplet Biogenesis Protects Mitochondrial Function during Starvation-Induced Autophagy. *Developmental Cell*, **42**(1), 9–21.

Petrella LN, Smith-Leiker T, Cooley L. (2007). The Ovhts polyprotein is cleaved to produce fusome and ring canal proteins required for Drosophila oogenesis. Development. 134, 703-12. doi: 10.1242/dev.02766.

Rambold, A. S., et al. (2015). Fatty acid trafficking in starved cells: regulation by lipid droplet lipolysis, autophagy, and mitochondrial fusion dynamics. *Developmental Cell*, **32**, 678–692.

Roshandel D, Sanders EJ, Shakeshaft A, Panjwani N, Lin F, Collingwood A, Hall A, Keenan K, Deneubourg C, Mirabella F, Topp S, Zarubova J, Thomas RH, Talvik I, Syvertsen M, Striano P, Smith AB, Selmer KK, Rubboli G, Orsini A, Ng CC, Møller RS, Lim KS, Hamandi K, Greenberg DA, Gesche J, Gardella E, Fong CY, Beier CP, Andrade DM, Jungbluth H, Richardson MP, Pastore A, Fanto M, Pal DK, Strug LJ; BIOJUME Consortium.(2023).

SLCO5A1 and synaptic assembly genes contribute to impulsivity in juvenile myoclonic epilepsy. NPJ Genom Med. 2023 Sep 28;8(1):28. doi: 10.1038/s41525-023-00370-z.

Sahut-Barnola I, Godt D, Laski FA, Couderc JL. (1995). Drosophila ovary morphogenesis: analysis of terminal filament formation and identification of a gene required for this process. Dev Biol. 170, 127-35. doi: 10.1006/dbio.1995.1201.

Sarikaya DP, Belay AA, Ahuja A, Dorta A, Green DA 2nd, Extavour CG. (2011). The roles of cell size and cell number in determining ovariole number in Drosophila. Dev Biol. 363, 279-89. doi: 10.1016/j.ydbio.2011.12.017.

Scanlan JL, Robin C, Mirth CK. (2023) Rethinking the ecdysteroid source during Drosophila pupal-adult development. Insect Biochem Mol Biol. 152:103891. doi: 10.1016/ j.ibmb.2022.103891.

Slaidina M, Banisch TU, Gupta S, Lehmann R. A single-cell atlas of the developing *Drosophila* ovary identifies follicle stem cell progenitors. Genes Dev. 2020 Feb 1;34(3-4):239-249. doi: 10.1101/gad.330464.119.

Slaidina M, Gupta S, Banisch TU, Lehmann R. A single-cell atlas reveals unanticipated cell type complexity in *Drosophila* ovaries. Genome Res. 2021 Oct;31(10):1938-1951. doi: 10.1101/gr.274340.120. Epub 2021 Aug 13. PMID: 34389661; PMCID: PMC8494228.

Song X, Call GB, Kirilly D, Xie T. (2007). Notch signaling controls germline stem cell niche formation in the Drosophila ovary. Development. 134, 1071-80. doi: 10.1242/dev.003392.

Svoboda M, Mungenast F, Gleiss A, Vergote I, Vanderstichele A, Sehouli J, Braicu E, Mahner S, Jäger W, Mechtcheriakova D, Cacsire-Tong D, Zeillinger R, Thalhammer T, Pils D. (2018). Clinical Significance of Organic Anion Transporting Polypeptide Gene Expression in

High-Grade Serous Ovarian Cancer. Front Pharmacol. 9, 842. doi: 10.3389/fphar.2018.00842.

Torrie, L.S., Radford, J.C., Southall, T.D., Kean, L., Dinsmore, A.J., Davies, S.A., Dow, J.A. (2004). Resolution of the insect ouabain paradox. Proc. Natl. Acad. Sci. U.S.A. 101(37): 13689--13693.

Zhu C-H, Xie T. (2003). Clonal expansion of ovarian germline stem cells during niche formation in Drosophila. Development 130, 2579-2586.

FIGURE LEGENDS

Figure 1. Localization of lipid droplets and Hts-positive aggregates in the terminal filament of the germarium.

(A) Schematic diagram of the germarium, highlighting the terminal filament (TF) at the anterior tip where germline stem cells (GSCs) reside.

(B–C) Lipid droplets (LDs), visualized using the neutral lipid dye BODIPY493/503 (arrow), detected within TF cells from day 1 to day 8 post-eclosion. Hts immunostaining reveals the presence of Hts-positive aggregates (orange triangle) within TF cells at early stages (day 0–1).

(D-F) LDs were observed throughout the germarium using BODIPY493/503, Nile Red, and LipidTOX staining.

(G) Number and size of LD within the TF, (H) Size of Hts aggregates ranging from 0.2 to 1.2 µm.

Figure 2. Terminal filament delivers lipids to germ cells through exocyst-dependent vesicle trafficking.

(A) Wild- type ovaries in driver line bab1-GAL4.

(B) Disrupted follicle development upon TF-specific *Sec6* knockdown using *bab1-GAL4.*

(C) Egg laying assay showing a significant reduction in the number of eggs produced per female per day following *Sec6* knockdown with *bab1-GAL4*.

(D-O) BODIPY 493/503 staining. **(D)** control germarium shows normal lipid droplet (LD) distribution.

(E) Conditional knockdown of *Sec6* in terminal filament cells using the *bab1-GAL4, tub-Gal80*^{ts} system (RNAi induced at late pupal stage, 29 °C) results in substantial depletion of lipid droplets in the germarium by day 8 post-eclosion.

(F) Quantification of LD number in control vs. *Sec6* knockdown, showing a significant decrease in LD abundance.

(G) Control germarium showing normal LD levels in TF and cap cells.

(H) *Sec6* knockdown leads to accumulation of enlarged LDs in TF and cap cells, indicating impaired lipid export due to disrupted exocytosis.

(I) Quantitative analysis reveals a significant increase in LD number and size within the TF following *Sec6* knockdown.

(J) Control germarium stained for LaminC (TF marker), BODIPY (LDs), and DAPI (nuclei), showing LDs distributed throughout the germarium.

(K-O) TF-specific knockdown of additional exocyst components *Sec15*, *Sec10*, *Sec5*, *Exo70*, and *Exo84* results in LD depletion in the germarium, showing the role of vesicle trafficking in lipid transport from the TF.

(P) Quantitative comparison of LD numbers across knockdowns of individual exocyst components, all showing reduced lipid levels in the germarium relative to controls.

Figure 3. Terminal filament dependent transport of lipids and cytoskeletal component supports germ cell and cyst development.

(A) Control germarium showing normal distribution of lipid droplets (LDs) throughout the germarium.

(B–E) LD staining (BODIPY 493/503) of germarium at days 2, 4, 6, and 8 post-eclosion following *Sec6* knockdown in terminal filament (TF) cells using *bab1-GAL4, tub-GAL80^ts*, with temperature shift to 29 °C at the late pupal stage. LDs accumulate within the TF, while their levels are markedly reduced in germ cells.

(B'–E') Hts staining shows progressive accumulation of Hts-positive cytoskeletal aggregates in TF cells from day 2 to 8, these aggregates are absent in control germarium **(A')**.

(F) Quantification of LD content in the TF following *Sec6* knockdown confirms significantly elevated lipid levels across time points.

(G) LD quantification in the germarium shows consistent depletion following *Sec6* knockdown relative to controls.

(H) Quantification of the number of Hts-positive aggregates per TF at days 2, 4, 6, and 8 post-eclosion indicates a progressive increase.

(I) Measurement of Hts aggregate size shows enlargement over time in *Sec6*-depleted TF cells.

(J) FM1-43 dye staining in control germaria shows strong signal in TF and cap cells, indicative of active vesicle trafficking and membrane recycling.

(K) FM1-43 staining is markedly reduced in TF and cap cells following *Sec6* knockdown, suggesting impaired exocytosis.

(L) Quantitative analysis of FM1-43 fluorescence intensity confirms a significant reduction in TF/cap cells in *Sec6* knockdown samples compared to controls.

(N) *Sec6* knockdown in escort cells driven by c587-GAL4 disrupts cyst and follicle formation, but LD levels in germ cells remain largely unaffected, compared to control (M).

(O) Quantification of LD signal in germ cells shows no significant difference between control and escort cell specific *Sec6* knockdown, supporting a limited role for escort cells in lipid transport.

(Q) Knockdown of *Hts* in germ cells disrupts fusome structure and reduces lipid droplet content, compared to control germarium **(P)**.

(R-T) Quantification confirms a significant decrease in LDs in germ cells upon fusome disruption, suggesting a fusome-associated role in lipid metabolism.

Figure 4: Oatp30B-mediated solute transport in the terminal filament regulates lipid delivery and germ cell differentiation.

(A) β-galactosidase staining from the PZ00078 Oatp30B-LacZ enhancer trap line shows strong expression localized to the terminal filament and cap cells.

(B–C) Lipid droplets labeled with BODIPY 493/503 in control (B) and Oatp30B knockdown germarium using *bab1-GAL4, tub-GAL80*^{ts} with RNAi induced at 29 °C late pupal stage, and dissected on day 7. Knockdown of Oatp30B results in a marked reduction of LDs and increase in spectrosome-like structures in germ cells.

(D) Quantification of LD levels reveals significant depletion in the germarium following *Oatp30B* knockdown compared to controls.

(E) Quantification of spectrosome-containing GSCs reveals an elevated number per germarium following Oatp30B knockdown, supporting a differentiation delay.

(F–G) Immunostaining with anti-Atp α reveals strong enrichment of Na^+/K^+-ATPase in terminal filament cells of control ovaries.

(H–I) TF-specific knockdown of *Oatp30B* significantly reduces Na^+/K^+-ATPase levels, suggesting impaired regulation of ion pump expression or stability.

(J–K) Hedgehog (Hh) staining shows robust expression in TFs of control ovaries (J), which is dramatically reduced upon *Oatp30B* knockdown (K).

(L) Quantification of Hh fluorescence intensity in the TF confirms a significant decline in signal following *Oatp30B* depletion, indicating compromised niche signaling.

Figure 5. Lipid droplets protect early germ cells from mitochondrial ROS accumulation.

(A) Control germarium showing close association of lipid droplets (BODIPY 493/503) with mitochondria (CytoC).

(B–C) Control (B) and germ cell-specific ACC knockdown (C) ovaries (using *nanos-GAL4*), showing severe loss of LDs upon depletion of the lipogenic enzyme Acetyl-CoA Carboxylase.

(D) Quantification of LD levels in germ cells shows a significant reduction following ACC knockdown.

(E–G) MitoSOX staining reveals elevated mitochondrial ROS in ACC knockdown (F) and TF-specific Sec6 knockdown (G), compared to control (E).

(H) Quantification of MitoSOX signal intensity shows significant ROS increase in both ACC- and Sec6-depleted germaria.

(I–K) DHE staining detects increased ROS levels in ACC knockdown (J) and TF-Sec6 knockdown (K) germaria relative to control (I).

(L) Quantification of DHE signal intensity confirms significantly elevated ROS in both experimental conditions, supporting a protective role for LDs against oxidative stress.

Figure 6. Hypothetical model illustrating the role of terminal filament cells in intercellular transport.

Terminal filament (TF) cells actively uptake precursor molecules from the surrounding haemolymph, process or package them, and deliver essential cargo including lipids, cytoskeletal

components, and organic solutes to underlying germ cells via vesicle-mediated trafficking and transporter activity.

(B–C) Control (B) and germ cell-specific ACC knockdown (C) ovaries (using *nanos-GAL4*), showing severe loss of LDs upon depletion of the lipogenic enzyme Acetyl-CoA Carboxylase.

(D) Quantification of LD levels in germ cells shows a significant reduction following ACC knockdown.

(E–G) MitoSOX staining reveals elevated mitochondrial ROS in ACC knockdown (F) and TF-specific Sec6 knockdown (G), compared to control (E).

(H) Quantification of MitoSOX signal intensity shows significant ROS increase in both ACC- and Sec6-depleted germaria.

(I–K) DHE staining detects increased ROS levels in ACC knockdown (J) and TF-Sec6 knockdown (K) germaria relative to control (I).

(L) Quantification of DHE signal intensity confirms significantly elevated ROS in both experimental conditions, supporting a protective role for LDs against oxidative stress.

Fig 6: Hypothetical model illustrating the role of terminal filament cells in intercellular transport.

Terminal filament (TF) cells actively uptake precursor molecules from the surrounding haemolymph, process or package them, and deliver essential cargo including lipids, cytoskeletal components, and organic solutes to underlying germ cells via vesicle-mediated trafficking and transporter activity.

SUPPLEMENTAL MATERIALS

Supplemental Tables

Table S1. Transporter and ion channel genes expressed in the adult TF

Gene	Avg_log2FC	p_val
Oatp30B (Organic anion transporter)	4.18	9.58E-07
CG4462 (Oganic anion transporter)	7.21	3.96E-04
Pmp70 (long-chain fatty acid transmembrane transporter)	2.72	3.93E-04
CG33970/Oskyddad (ABC-type transporter)	4.96	1.79E-11
ATP8B (P-type phospholipid transporter	5.46	3.50E-13
Slo (Calcium-activated potassium channel)	10.36	3.25E-38
CG6928 (chloride and sulfate transmembrane transporter)	6.09	2.62E-23
CG4587/Stolid (Voltage-gated calcium channel)	6.42	9.51E-14
shakB (Monoatomic ion transmembrane transporter)	6.42	9.51E-14
CG34396 (potassium ion transmembrane transporter)	4.93	2.36E-07
CG42817 (Calcium ion transmembrane transport)	5.58	3.33E-05
Shaw (Voltage-gated potassium channel)	3.49	3.48E-05
Drip (Transport of water across cell membrane)	10.59	3.25E-38

Table S1. A list of genes annotated as transporter or ion channels that are expressed in the adult terminal filament.

Supplemental Figure Legends

Fig S1: Lipid droplet accumulation in the terminal filament persists across aging following *Sec6* knockdown.

(A–G) BODIPY 493/503 staining of germaria at days 1, 10, 20, and 30 post-eclosion in *bab1-GAL4, tub-GAL80^{ts} > Sec6-RNAi* flies (RNAi induced at 29 °C lat ate pupal stage), showing persistent lipid droplet accumulation in the terminal filament over time.

(H, I) Quantification of LD number and size in TFs across aging stages reveals sustained lipid buildup, indicating a stable defect in lipid trafficking that is not diminished by age-related TF remodeling.

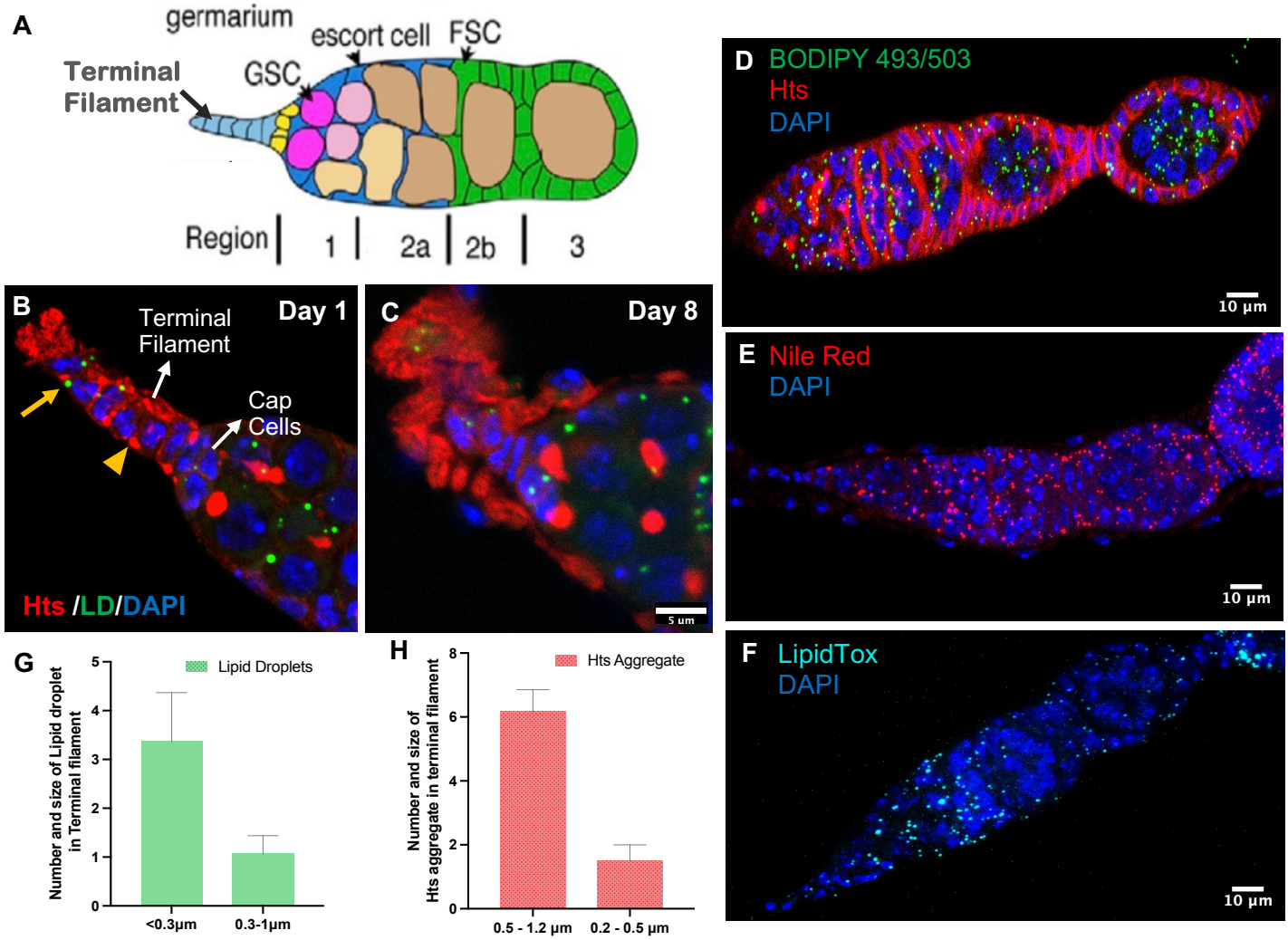
A
germarium
escort cell
FSC
Terminal Filament
GSC
Region
1
2a
2b
3
B
Day 1
Terminal Filament
Cap Cells
Hts /LD/DAPI
C
Day 8
5 um
D
BODIPY 493/503
Hts
DAPI
10 µm
E
Nile Red
DAPI
10 µm
F
LipidTox
DAPI
10 µm
G
Lipid Droplets
Number and size of Lipid droplet in Terminal filament
<0.3µm
0.3-1µm
H
Hts Aggregate
Number and size of Hts aggregate in terminal filament
0.5 - 1.2 µm
0.2 - 0.5 µm

Fig. 1

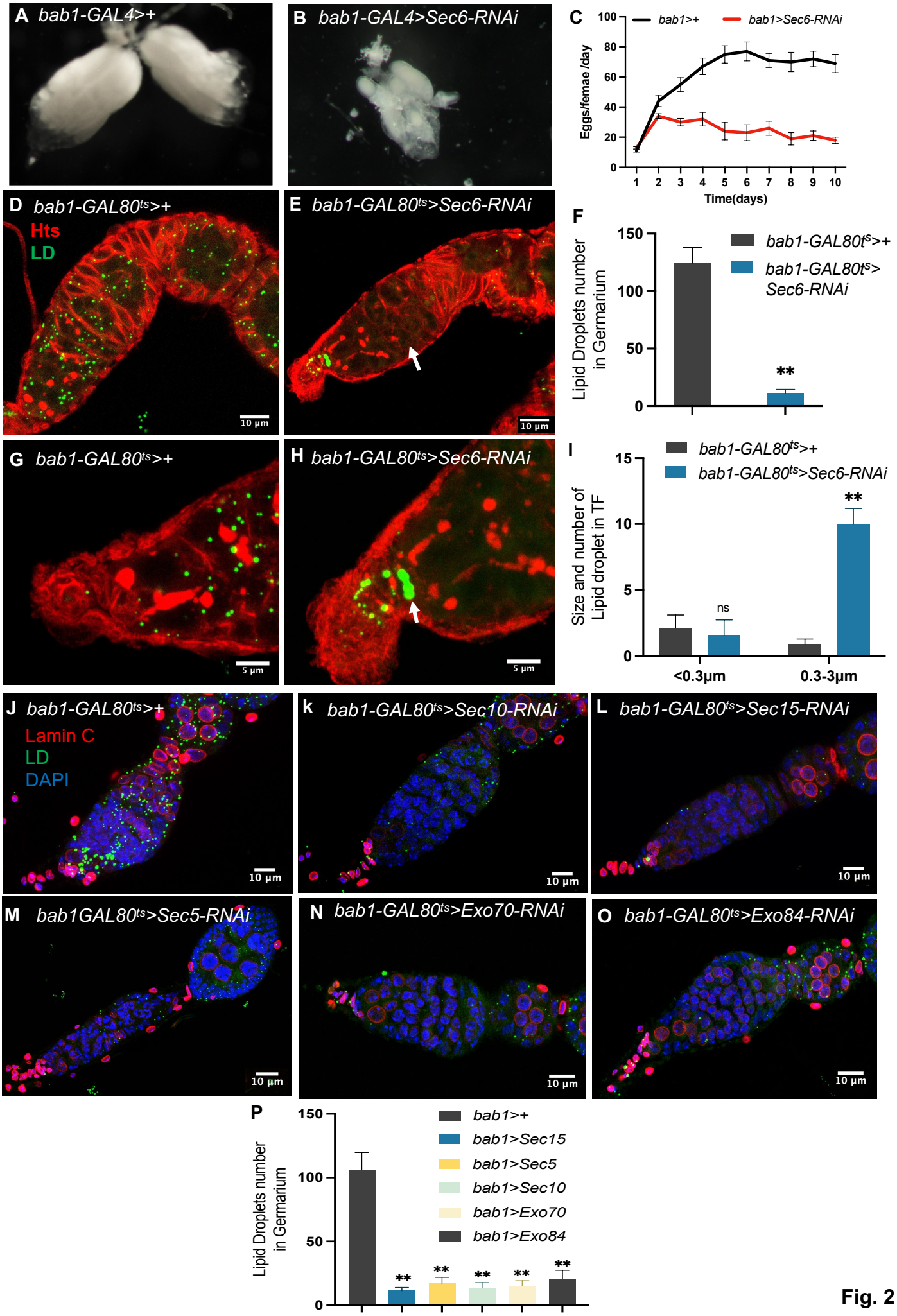
A bab1-GAL4>+
B bab1-GAL4>Sec6-RNAi
C
bab1>+
bab1>Sec6-RNAi
Eggs/femae /day
Time(days)
D bab1-GAL80ts>+
Hts
LD
10 μm
E bab1-GAL80ts>Sec6-RNAi
10 μm
F
Lipid Droplets number in Germarium
bab1-GAL80ts>+
bab1-GAL80ts> Sec6-RNAi
**
G bab1-GAL80ts>+
5 μm
H bab1-GAL80ts>Sec6-RNAi
5 μm
I
bab1-GAL80ts>+
bab1-GAL80ts>Sec6-RNAi
Size and number of Lipid droplet in TF
ns
**
<0.3μm
0.3-3μm
J bab1-GAL80ts>+
Lamin C
LD
DAPI
10 μm
k bab1-GAL80ts>Sec10-RNAi
10 μm
L bab1-GAL80ts>Sec15-RNAi
10 μm
M bab1GAL80ts>Sec5-RNAi
10 μm
N bab1-GAL80ts>Exo70-RNAi
10 μm
O bab1-GAL80ts>Exo84-RNAi
10 μm
P
Lipid Droplets number in Germarium
bab1>+
bab1>Sec15
bab1>Sec5
bab1>Sec10
bab1>Exo70
bab1>Exo84
**

Fig. 2

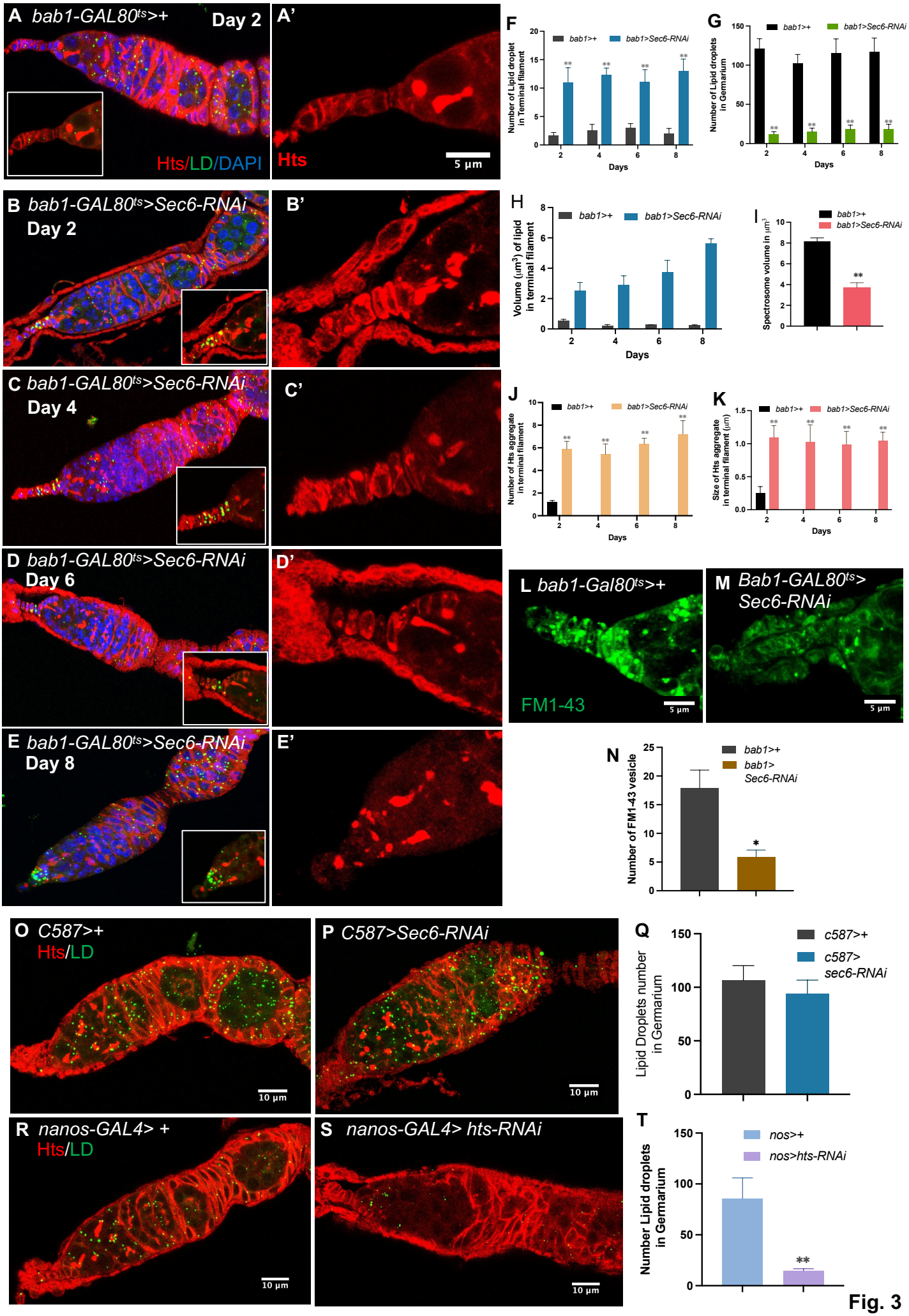
A bab1-GAL80ts>+
Day 2
Hts/LD/DAPI
A'
Hts
5 µm
B bab1-GAL80ts>Sec6-RNAi
Day 2
B'
C bab1-GAL80ts>Sec6-RNAi
Day 4
C'
D bab1-GAL80ts>Sec6-RNAi
Day 6
D'
E bab1-GAL80ts>Sec6-RNAi
Day 8
E'
F
bab1>+
bab1>Sec6-RNAi
Number of Lipid droplet in Terminal filament
Days
G
Number of Lipid droplets in Germarium
H
Volume (µm3) of lipid in terminal filament
I
Spectrosome volume in µm3
J
Number of Hts aggregate in terminal filament
K
Size of Hts aggregate in terminal filament (µm)
L bab1-Gal80ts>+
FM1-43
M Bab1-GAL80ts> Sec6-RNAi
N
Number of FM1-43 vesicle
bab1>+
bab1> Sec6-RNAi
O C587>+
Hts/LD
P C587>Sec6-RNAi
10 µm
Q
Lipid Droplets number in Germarium
c587>+
c587> sec6-RNAi
R nanos-GAL4> +
Hts/LD
S nanos-GAL4> hts-RNAi
T
Number Lipid droplets in Germarium
nos>+
nos>hts-RNAi

Fig. 3

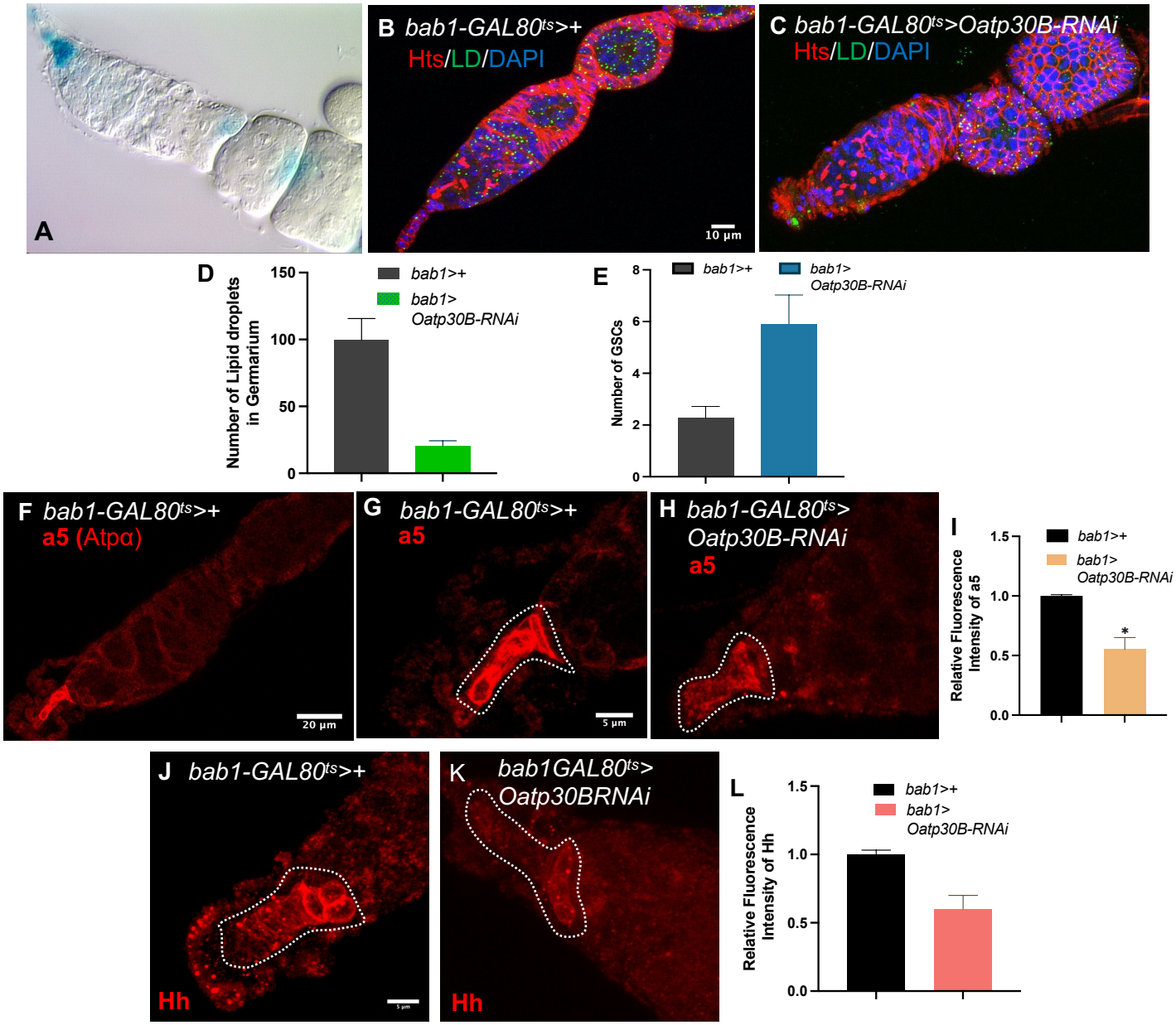
A
B bab1-GAL80ts>+
Hts/LD/DAPI
10 µm
C bab1-GAL80ts>Oatp30B-RNAi
Hts/LD/DAPI
D
Number of Lipid droplets in Germarium
150
100
50
0
bab1>+
bab1> Oatp30B-RNAi
E
Number of GSCs
8
6
4
2
0
bab1>+
bab1> Oatp30B-RNAi
F bab1-GAL80ts>+
a5 (Atpα)
20 µm
G bab1-GAL80ts>+
a5
5 µm
H bab1-GAL80ts> Oatp30B-RNAi
a5
I
Relative Fluorescence Intensity of a5
1.5
1.0
0.5
0.0
bab1>+
bab1> Oatp30B-RNAi
*
J bab1-GAL80ts>+
Hh
K bab1GAL80ts> Oatp30BRNAi
Hh
L
Relative Fluorescence Intensity of Hh
1.5
1.0
0.5
0.0
bab1>+
bab1> Oatp30B-RNAi

Fig. 4

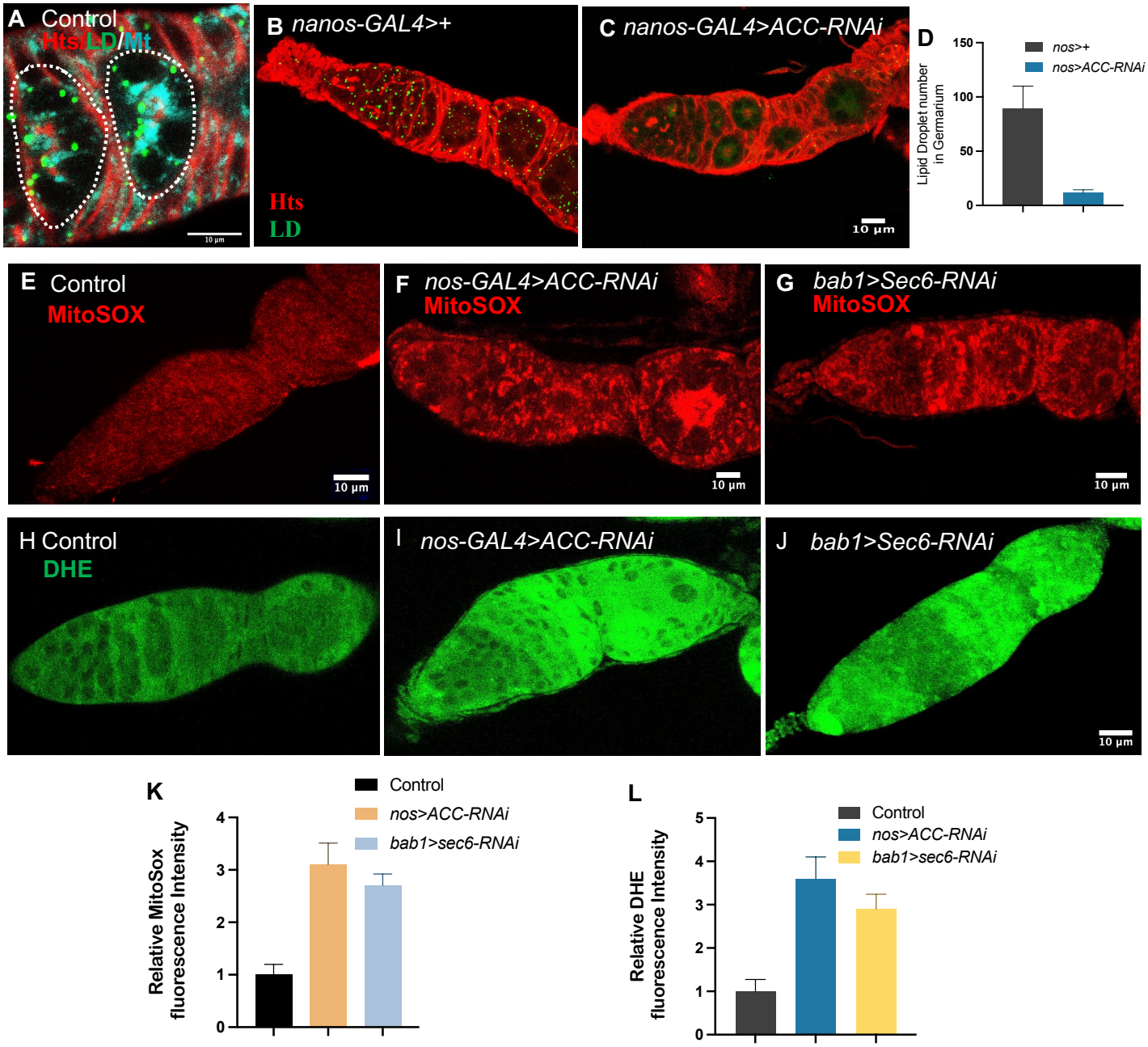
A Control
Hts/LD/Mt
10 µm
B nanos-GAL4>+
Hts
LD
C nanos-GAL4>ACC-RNAi
10 µm
D
Lipid Droplet number in Germarium
150
100
50
0
nos>+
nos>ACC-RNAi
E Control
MitoSOX
10 µm
F nos-GAL4>ACC-RNAi
MitoSOX
10 µm
G bab1>Sec6-RNAi
MitoSOX
10 µm
H Control
DHE
I nos-GAL4>ACC-RNAi
J bab1>Sec6-RNAi
10 µm
K
Relative MitoSox fluorescence Intensity
4
3
2
1
0
Control
nos>ACC-RNAi
bab1>sec6-RNAi
L
Relative DHE fluorescence Intensity
5
4
3
2
1
0
Control
nos>ACC-RNAi
bab1>sec6-RNAi

Fig.5

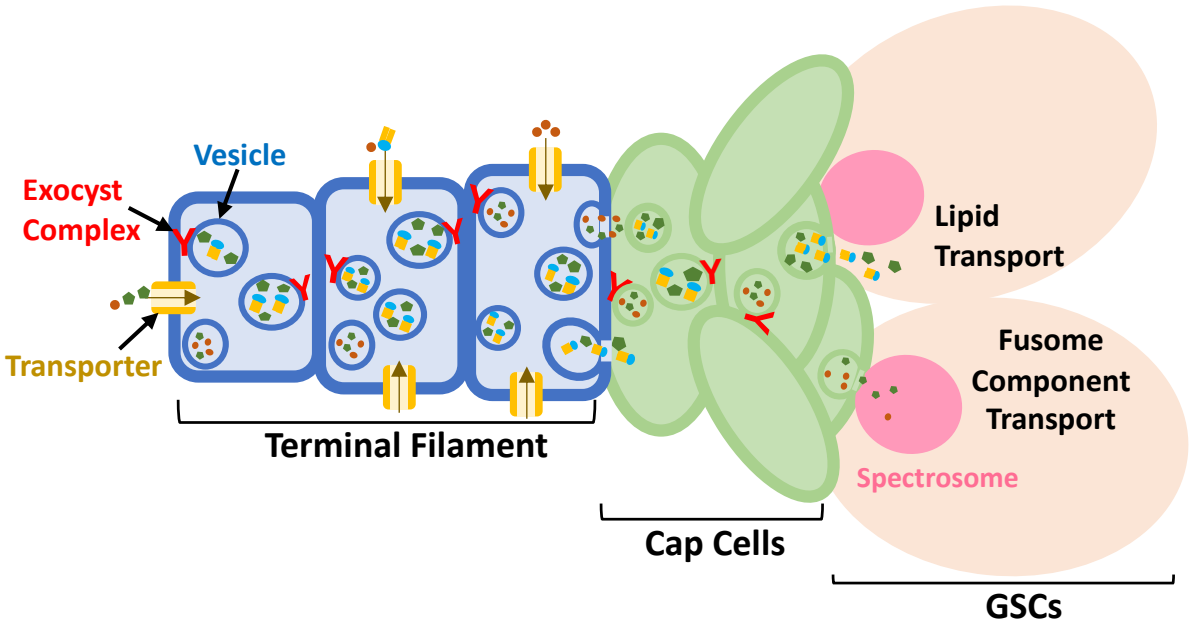
Vesicle
Exocyst
Complex
Transporter
Terminal Filament
Cap Cells
GSCs
Lipid
Transport
Fusome
Component
Transport
Spectrosome

Fig.6